

S3TC: Spiking Separated Spatial and Temporal Convolutions with Unsupervised STDP-based Learning for Action Recognition

Mireille El-Assal*, Pierre Tirilly*, and Ioan Marius Bilasco*

* Univ. Lille, CNRS, Centrale Lille, UMR 9189 CRISTAL, F-59000 Lille, France

Email: mireille.elassal2@univ-lille.fr, pierre.tirilly@univ-lille.fr, marius.bilasco@univ-lille.fr

Abstract—Video analysis is a major computer vision task that has received a lot of attention in recent years. The current state-of-the-art performance for video analysis is achieved with Deep Neural Networks (DNNs) that have high computational costs and need large amounts of labeled data for training. Spiking Neural Networks (SNNs) have significantly lower computational costs (thousands of times) than regular non-spiking networks when implemented on neuromorphic hardware [1], [2]. They have been used for video analysis with methods like 3D Convolutional Spiking Neural Networks (3D CSNNs). However, these networks have a significantly larger number of parameters compared with spiking 2D CSNN. This, not only increases the computational costs, but also makes these networks more difficult to implement with neuromorphic hardware. In this work, we use CSNNs trained in an unsupervised manner with the Spike Timing-Dependent Plasticity (STDP) rule, and we introduce, for the first time, Spiking Separated Spatial and Temporal Convolutions (S3TCs) for the sake of reducing the number of parameters required for video analysis. This unsupervised learning has the advantage of not needing large amounts of labeled data for training. Factorizing a single spatio-temporal spiking convolution into a spatial and a temporal spiking convolution decreases the number of parameters of the network. We test our network with the KTH, Weizmann, and IXMAS datasets, and we show that S3TCs successfully extract spatio-temporal information from videos, while increasing the output spiking activity, and outperforming spiking 3D convolutions.

Index Terms—spiking neural networks, STDP, action classification, 3D convolution, spatial, temporal, separated convolutions.

I. INTRODUCTION

A large amount of new visual data is made available to the world on a daily basis, with a substantial portion of this data comprising videos. Analyzing this large amount of data is challenging for humans, which has rendered video analysis an important computer vision task. Deep learning methods achieve state-of-the-art performance for visual data analysis. However, their computational cost is very high, which makes using them on energy-constrained devices very challenging. Moreover, training them needs large amounts of labeled data, which requires costly human intervention to create. This has pushed forward the exploration of methods that can analyze visual data at a lower cost. Among these methods are Spiking Neural Networks (SNNs), which are third generation neural networks that can process visual information in the form of low-energy spikes [2]. They carry potential benefits such as

fast information processing when implemented on neuromorphic hardware and energy efficiency [2]–[4], which encourages their use for video analysis.

There are some spiking models proposed for video analysis, including spiking two-stream methods [5], spiking ResNets [6], 2D Convolutional Spiking Neural Network (CSNN) and 3D CSNN [7]. While most spiking methods, similarly to 2D CSNNs, require non-spiking processes [8] for motion extraction, 3D CSNNs [7] have the advantage of being fully spiking solutions for learning motion patterns. However, similarly to traditional methods, spiking 3D convolutions increase the number of trainable parameters with respect to spiking 2D convolutions. This can make it more challenging to implement this model on neuromorphic hardware, as having more parameters results in a greater number of connections that need to be constructed in the hardware implementation. Consequently, this increases the computational costs of these networks as compared to 2D CSNNs. Therefore, there is a need to develop methods that can reduce the number of parameters while conserving the ability to directly learn spatio-temporal patterns. Separated convolution could be one solution, that has been used with CNNs [9]–[11], but has not yet been used in the spiking domain.

In this work, we present Spiking Separated Spatial and Temporal Convolutions (S3TCs), where we reduce the number of parameters in a spiking spatio-temporal 3D convolution by factorizing it into two separate smaller spatial and temporal convolutions. We use CSNNs trained with the unsupervised Spike Timing-Dependent Plasticity (STDP) learning rule. S3TCs are expected to be more efficient and hardware friendlier solutions. To the best of our knowledge, our work is the first to address the subject of separated convolutions with spiking neural networks. We hypothesize that the benefits of separated convolutions with CNNs could apply to SNNs, and that simpler filters, or smaller filter sizes, can improve STDP-based learning by capturing more patterns and prompting the neurons to fire more spikes. As STDP updates occur upon neurons firing spikes, this increased activity can result in more updates, making learning more effective.

This work is a building block towards improving the performance of spiking models that can learn spatio-temporal features. The main contributions of this paper are summarized as follows:

- we present Spiking Separated Spatial and Temporal Con-

volution (S3TCs);

- we evaluate the performance of S3TC models with different filter sizes on the KTH [12], Weizmann [13], and IXMAS [14] datasets;
- we compare the performance of S3TCs to that of spiking 3D convolution from [7], and we conclude that S3TCs can achieve better performance;
- we show that smaller filter sizes, to a certain extent with STDP, prompt the neurons to fire more spikes, thus increasing the network activity and improving the learning.

II. RELATED WORK

3D CNNs are a common practice for motion modeling [15]–[20]. The third dimension of these networks, which is devoted to time, enables the extraction of spatio-temporal features. In [21], the authors present deep 3D CNNs for spatio-temporal feature learning. They compare them to 2D CNNs, and conclude that 3D architectures perform better for video analysis. However, these models still have many issues. For instance, they have more trainable parameters than 2D models, which consequently increases their computational cost and makes the optimization of these parameters more difficult. Moreover, these models are energy-consuming and require powerful GPUs to run efficiently. Running them on devices with limited energy is very challenging. The environmental concerns of running powerful GPUs for extended periods of time [22], [23] motivated the search for alternative methods that have lower computational costs, one of which is separable convolutions. With separable convolutions, a large convolution filter is separated into two or more smaller filters. Separable convolutions adopted in networks like MobileNets [10] and Xception [24] have succeeded in decreasing the number of parameters of these networks while preserving their performance. Moreover, gains in accuracy have been recorded when factorizing a 3D convolution into a 2D spatial convolution and a 1D temporal convolution [25]. In [25], the authors attribute this gain in accuracy to additional nonlinearities added by the separated convolutions compared to using a 3D convolution. They argue that these nonlinearities render the model capable of representing more complex functions. They also add that 2D and 1D filters are easier to optimize than 3D filters, where appearance and dynamics are intertwined. However, none of the neural networks discussed up until this point are spiking models.

CSNNs provide a cost-effective and unsupervised alternative for motion modeling. 3D CSNNs have been proposed recently [7]. In [7], the authors use unsupervised STDP-based 3D CSNNs, and conclude that 3D CSNNs outperform 2D CSNNs for the task of human action recognition, especially with longer video sequences. However, despite the energy efficiency of these 3D CSNN models compared with traditional non-spiking methods, the additional parameters, with regard to 2D CSNNs, result in higher costs and potentially more complex neuromorphic hardware [26]. As previously mentioned, spiking-separable convolutions have not yet been explored in the literature. However, they are excellent candidates for efficient hardware-friendly video analysis models.

III. BACKGROUND & NETWORK ARCHITECTURE

This section contains the needed background information and mechanisms chosen for achieving S3TCs with unsupervised STDP learning. This includes a simplified explanation of 3D CSNNs from [7], and a discussion of the number of parameters required to train this network.

A. A video sample

A video is a frame sequence represented as a 4D tensor of size $l_w \times l_h \times l_c \times l_{td}$ where l_w and l_h are the width and height of the frames, l_c is their number of channels, which is 1 in the case of gray scale frames, and l_{td} is the temporal depth of the tensor i.e., the number of frames in the video sample.

B. Neuron model and training

The CSNNs used in this work consist of one feed-forward layer that contain Integrate-and-Fire (IF) neurons [27]. The IF neuron model is characterized by having a certain membrane potential $v(t)$ and a threshold potential $v_{th}(t)$. Input spikes are integrated into the neuron’s membrane potential until it reaches its threshold, thereby triggering the neuron to generate an output spike. Then, the membrane potential is reset to its resting potential v_r , which is 0 volts in this work. Specifically, we have built upon the network architecture of [7] and utilized the same neuron model and threshold adaptation mechanisms. This decision was made to ensure an accurate comparison of the performance between our S3TC and the 3D convolution model presented in [7].

Training is unsupervised and uses the biological STDP learning rule [28]. This is a local learning rule that acts on a synapse connecting two neurons at a time. Therefore, it is not affected by changes in the network architecture. These networks use Winner-Takes-All (WTA) inhibition during training to prevent several neurons from learning the same pattern. With WTA, some neurons can overpower other neurons, i.e., they have a tendency to fire more spikes than others. This leads to the network becoming stuck in a state where a few active neurons fire all the time, while the other neurons are quiet. In order to ensure the stability of the network, we use the threshold adaptation method introduced in [3]. This method trains the neurons to fire at a given target timestamp \hat{t} , which controls the patterns learned by the network, and promotes the activity of all neurons. Within this method, each time a neuron fires or receives an inhibitory spike, the thresholds of all neurons (winners and losers) are adapted so that their firing time converges rapidly towards \hat{t} . Furthermore, the threshold of the neuron that fired is raised, while the thresholds of all the other neurons are lowered, with the aim of encouraging their activation.

C. 3D convolution

A 3D convolutional layer has f_k trainable filters, with sizes $f_w \times f_h \times f_{td}$, where f_w and f_h represent the width and height of the filter respectively, and f_{td} is the temporal size of the filter. These filters can slide along the temporal dimension of a video sample, in addition to the spatial ones.

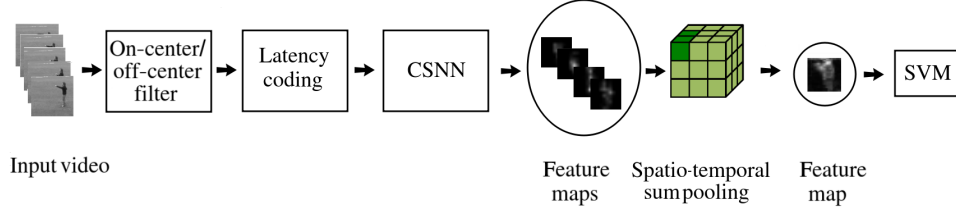


Fig. 1. Pipeline for action recognition with unsupervised feature learning by an SNN.

Each neuron of a layer is connected to $f_w \times f_h \times f_{td}$ neurons of the previous layer. 3D spiking convolution can be formalized as shown in Equations 1 and 2 from [7]:

$$f_s(x) = \begin{cases} 1, & \text{if } x \geq 0 \\ 0, & \text{otherwise} \end{cases} \quad (1)$$

$$v_{x,y,z,k}(t) = \sum_{n \in \mathcal{N}} W_{i(x_n),j(y_n),m(z_n),k_n,k} \times f_s(t - t_n) \quad (2)$$

where f_s is the kernel of spikes, $v(t)$ is the potential of the neuron membrane at time t , and x, y, z , and k are the coordinates of the spike in the width, height, time, and channel dimensions, respectively. \mathcal{N} is the set of input connections in the neighborhood, $W \sim U(0, 1)$ is the trainable synaptic weight matrix, $i()$, $j()$, and $m()$ are functions that are used to map the location of the input neuron to the corresponding location in the weight matrix, and k is the index of the trainable filter. When the membrane potential $v_{x,y,z,k}(t)$ crosses the threshold potential $v_{th}(t)$, the synaptic weights and thresholds of the network are updated.

The number of parameters required for training a spiking 3D CSNN is:

$$|P| = f_k \times n_c \times f_w \times f_h \times f_{td} \quad (3)$$

where P represents the set of parameters in the model, f_k is the number of filters, n_c is the number of input channels, f_w and f_h represent the width and height of the filter, respectively, and f_{td} is the temporal size of the filter.

D. Baseline architecture

The baseline architecture is shown in Figure 1. The video frames are filtered with an on-center/off-center filter [29], which uses a Difference-of-Gaussian (DoG) filter used to pre-process the data by simulating on-center/off-center cells and extracting edges. This filter is needed because STDP-based SNNs need edges to learn informative patterns [30]. After that, latency coding is applied to transform the edges into spikes represented by timestamps. High edge values are represented as early spikes, while low values come later. Next comes the CSNN processing, which can be a 3D CSNN as mentioned in Section III-C or a S3TC network. The output of our network will consist of spatio-temporal feature maps, which are then reduced in size using spatio-temporal sumpooling before being sent to the SVM for classification.

IV. SEPARATED SPATIAL & TEMPORAL CONVOLUTIONS

With separated convolutions, the filter connectivity of the spiking 3D convolution layer introduced in Section III-C can be broken down into two parts, space-wise and time-wise convolutions, as shown in Figure 2.

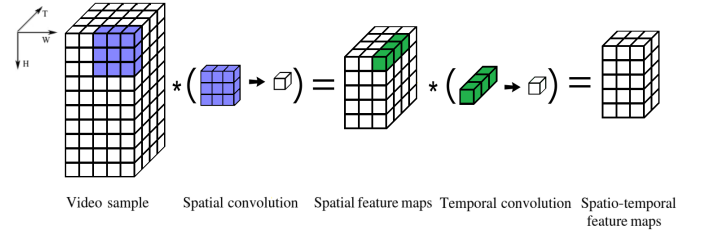


Fig. 2. Separable spatial and temporal convolutions.

In the first phase, a 2D filter crosses over the spatial dimension of the input, one frame at a time. This filter has a dimension of $f_w \times f_h \times 1$, and results in spatial feature maps. In the second phase, with the time-wise convolution, we compute a linear combination of the spatial feature maps by undergoing a $1 \times 1 \times f_{td}$ convolution in the temporal dimension to extract meaningful temporal information from the spatial feature maps. S3TC can be formalized as Equation 4 for the space-wise convolution, and Equation 5 for the time-wise convolution:

$$v_{x,y,k}(t) = \sum_{n \in \mathcal{N}_s} W_{i(x_n),j(y_n),k_n,k} \times f_s(t - t_n) \quad (4)$$

$$v_{z,k}(t) = \sum_{n \in \mathcal{N}_t} W_{m(z_n),k_n,k} \times f_s(t - t_n) \quad (5)$$

where f_s is the kernel of spikes, $v(t)$ is the potential of the neuron membrane at time t , and x, y, z , and k are the coordinates of the spike in the width, height, time, and channel dimensions, respectively. $W \sim U(0, 1)$ is the trainable synaptic weight matrix, $i()$, $j()$, and $m()$ are functions that are used to map the location of the input neuron to the corresponding location in the weight matrix, k is the index of the trainable filter, and \mathcal{N}_s and \mathcal{N}_t are the sets of input connections in the spatial and temporal neighborhoods, respectively.

The number of parameters required for training S3TCs becomes:

$$|P'| = f_k \times n_c \times (f_w \times f_h + f_{td}) \quad (6)$$

This number of parameters is lower than that of a spiking 3D convolution, therefore the computational cost of training S3TCs is lower than that of training spiking 3D convolutions. In the next section, we study the trade-off between accuracy and efficiency with these two spiking convolution settings.

V. EVALUATION

This section contains the details of our experiments. First, we present the datasets, along with the implementation details and the main parameters of our network. Then we present the results of implementing and testing our S3TCs, and we compare them to spiking 3D convolutions.

A. Datasets and evaluation protocol

We use three datasets, the KTH, Weizmann, and IXMAS datasets. The KTH and Weizmann datasets are early and simple datasets for action recognition. Although traditional computer vision approaches have already achieved high recognition rates on these datasets [31], their simplicity makes them good candidates to study the performance of new models like the ones targeted in this paper. The IXMAS dataset features different actors, cameras, and viewpoints, which adds complexity. Moreover, the settings are challenging, as two thirds of the recordings contain objects in the scene, partially occluding the actors.

The KTH dataset contains 600 videos that are made up of 25 subjects performing 6 actions in 4 scenarios. Subjects 11, 12, 13, 14, 15, 16, 17, and 18 are used for training, while 19, 20, 21, 23, 24, 25, 01, 04 are used for validation, and 02, 03, 05, 06, 07, 08, 09, 10, and 22 are used for testing, as indicated in the KTH protocol.

The Weizmann dataset contains 90 videos of 9 subjects performing 10 actions. The experiments on this dataset all use the leave-one-subject-out strategy.

The IXMAS action recognition dataset is made up of 10 subjects, 11 actions and 1148 sequences. The experiments on this dataset also use the leave-one-subject-out strategy.

To shorten the running time of experiments, we take subsets of the video frames, like in [20], [32], and [7]. We use 10 frames per video, and skip three frames between each two selected frames in order to make sure to capture a full cycle of the performed action. We also scale down the frame sizes to half of their original sizes to increase the processing speed.

We measure the classification accuracy (in %) on the test set for all experiments. Each experiment was run three times, and we report the average accuracy over the three runs.

B. Implementation details

The video is pre-processed with the on-center/off-center filter mentioned in III-D. This filter has a size of 7, and uses centered Gaussians of variance 1.0 and 4.0. The convolutional layer has $f_k = 64$ filters for both 3D and S3TC settings.

The neuron thresholds are randomly initialized with a normal distribution, which has a mean of 8 and variance of 0.1 for all experiments except those with a filter size of 3, where we decrease the mean to 7. This is because small filters integrate

fewer input spikes, resulting in no spiking activity when the threshold is too high.

The value of the target timestamp \hat{t} discussed in Section III-B are taken from [7]. We use a value of $\hat{t} = 0.65$ for the KTH and IXMAS datasets, and a value of $\hat{t} = 0.75$ for the Weizmann dataset. The spatio-temporal pooling is set to limit the size of the output feature maps to $20 \times 20 \times 2$.

Then the output feature maps are linearized and introduced into a Support Vector Machine (SVM) with a linear kernel, which performs action classification. Any other supervised method can be used for the final classification; we chose an SVM because it is standard and effective with default hyperparameters.

The software simulator used to simulate the convolutional SNNs tested in this work is the `csnn-simulator` [30], which is a publicly available and open-source simulator. The source code for our experiments will be released publicly as a specific branch of the `csnn-simulator` [30].

C. 3D vs. Separable convolutions

We test 3D convolutions and S3TCs for five different filter sizes. For the sake of limiting the possible filter size combinations, we use the same size $f = f_h = f_w = f_{td}$ for all dimensions. A 3D convolution has filters of size $f \times f \times f$, while the filter sizes of its corresponding separated convolutions are $f \times f \times 1$ for the spatial convolution and $1 \times 1 \times f$ for the temporal one. The most commonly used filter size is 3 [10], [11], [24]. However, larger filter sizes like 5 and 7 have shown to give better results in [33], so we include these filter sizes in our experiments.

Table I shows the results of the experiments. These results show that S3TCs can achieve better performance than 3D convolution, while having less parameters, and thus a lower computational cost. These results show that different datasets have different ideal filter sizes for S3TCs (7 for the KTH dataset, 3 for IXMAS, and 5 for Weizmann). These results also show that filter size has more impact on the results with S3TC; for instance, with the KTH dataset, changing the filter size from 3 to 7 using 3D convolutions has an impact of approximately +5*p.p.*, while with S3TCs, the impact is approximately +10*p.p.*

In the context of action recognition, the spatial filters are responsible for extracting interesting spatial features in successive frames. However, these filters alone cannot make sense of the relationship between these extracted feature maps. The 1D filters model the time dimension, thus combining the output feature maps of the 2D filters into more discriminant combinations that include motion. Larger temporal filters provide a better extraction of these moving patterns with datasets that exhibit significant variations or movements relative to the frame size, like the KTH dataset, while smaller filters are needed for datasets that exhibit smaller variations, like the Weizmann dataset. Therefore, the performance of S3TCs, similarly to 3D convolutions, depends greatly on choosing suitable hyperparameters.

With large enough filter sizes (e.g., 7 and 9), the S3TC method can outperform regular 3D convolutions for most

(A) Filter size = 3		
Dataset	3D Conv	Separated Conv
KTH	59.41 \pm 0.43	60.65 \pm 0.37
Weizmann	56.58 \pm 0.00	60.06 \pm 1.88
IXMAS	53.81 \pm 0.45	52.26 \pm 0.63
(B) Filter size = 5		
Dataset	3D Conv	Separated Conv
KTH	61.88 \pm 0.57	69.29 \pm 0.21
Weizmann	57.61 \pm 0.00	66.24 \pm 0.00
IXMAS	51.56 \pm 0.12	51.44 \pm 0.18
(C) Filter size = 7		
Dataset	3D Conv	Separated Conv
KTH	64.20 \pm 0.21	70.52 \pm 0.78
Weizmann	57.09 \pm 0.00	65.78 \pm 0.92
IXMAS	40.74 \pm 0.38	48.87 \pm 0.60
(D) Filter size = 9		
Dataset	3D Conv	Separated Conv
KTH	62.81 \pm 0.21	65.43 \pm 0.21
Weizmann	56.50 \pm 0.00	64.62 \pm 0.00
IXMAS	34.01 \pm 0.27	46.46 \pm 0.21
(E) Filter size = 10		
Dataset	3D Conv	Separated Conv
KTH	60.65 \pm 0.00	61.11 \pm 0.75
Weizmann	58.09 \pm 0.52	57.12 \pm 0.52
IXMAS	27.94 \pm 0.20	38.50 \pm 0.28

TABLE I

CLASSIFICATION RATES IN % (AVERAGE \pm STANDARD DEVIATION) FOR THE KTH, WEIZMANN, AND IXMAS DATASETS (10 FRAMES PER VIDEO) OVER 3 RUNS WITH 3D CONVOLUTION AND SEPARATED CONVOLUTIONS.

datasets. This behavior, where separated convolutions outperforms 3D convolutions, is similar to the one observed in [25], where they specify that 2D and 1D filters are easier to optimize with supervised learning than 3D filters.

In our case, this supervised weight optimization process does not happen with STDP, where we use unsupervised learning, and thus cannot be the reason for the amelioration in performance. In the case of a spiking model, we observe that more spikes are fired when using separated convolutions than its 3D counterpart, as shown in Figure 3. This is due to the simplicity of the 2D spatial and 1D temporal filters, which enables them to capture more pattern occurrences than the complex 3D filters. This results in firing a larger number of output spikes with S3TCs and increases the activity of the network. This yields less sparsity in the final vector fed into the SVM and more training updates with STDP, which results in a higher accuracy. This is consistent with previous observations that excessive sparsity can lower recognition performance [34].

VI. CONCLUSION

Spiking neural networks can offer an energy-efficient solution on neuromorphic hardware. However, using 3D convolutions, which are suitable for video analysis, increases the

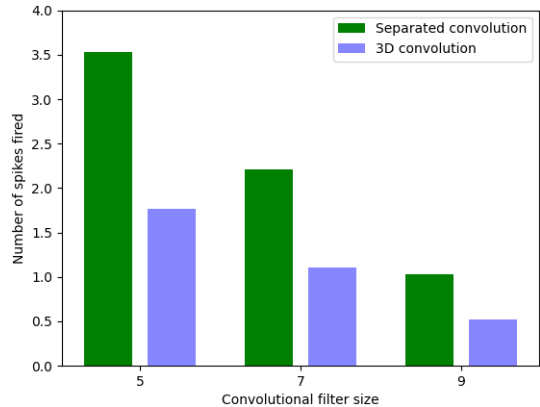


Fig. 3. The final output number of spikes fired by separable spatial and temporal convolutions compared to 3D convolutions with filter sizes of 5, 7 and 9 using the KTH dataset.

number of parameters, making training more challenging and potentially leading to more complex hardware requirements. To mitigate this issue, we chose to reduce the number of parameters in the network by replacing spiking 3D convolutions with spiking separated convolutions.

In this work, we factorize a single 3D spiking convolution into two separate spatial and temporal spiking convolutions. This separation decreases the number of parameters, and can improve the performance when using sufficiently large filters. The difference in performance between 3D convolutions and separable convolutions is highly dependent on choosing the appropriate hyperparameters (i.e., filter size).

Our first conclusion is that the optimum filter sizes vary from one dataset to another depending on their motion variations. A second conclusion is that S3TCs can outperform 3D convolutions due to the simplicity of their filters, which leads to capturing more patterns and thus firing more spikes. We believe that, with STDP, there is a proportional relationship between the number of input spikes in a layer and the quality of the learned filters. Additionally, the fact that S3TCs produce more output spikes makes them more advantageous than 3D CSNNs for constructing multi-layer spiking models, since activity loss is a major issue in deep SNNs [35].

A promising avenue for future work would involve using a multi-stream architecture with S3TC networks, each stream using a specific filter size. This approach would enable capturing information about both small and large motion patterns, resulting in better generalization across different datasets.

VII. ACKNOWLEDGMENTS

This work has been supported by IRCICA (USR 3380) under the bio-inspired project, and funded by Région Hauts-de-France.

REFERENCES

- [1] Yinqian Sun, Yi Zeng, and Yang Li. Solving the Spike Feature Information Vanishing Problem in Spiking Deep Q Network With Potential Based Normalization. *Frontiers in Neuroscience*, 16, 2022.
- [2] Amirhossein Tavaneai, Masoud Ghodrati, Saeed Reza Kheradpisheh, Timothée Masquelier, and Anthony Maida. Deep Learning in Spiking Neural Networks. *Neural Networks*, 111:47–63, 2019.

- [3] Pierre Falez, Pierre Tirilly, Ioan Marius Bilasco, Philippe Devienne, and Pierre Boulet. Multi-layered Spiking Neural Network with Target Timestamp Threshold Adaptation and STDP. In *International Joint Conference on Neural Networks (IJCNN)*, 2019.
- [4] Chankyu Lee, Priyadarshini Panda, G. Srinivasan, and K. Roy. Training Deep Spiking Convolutional Neural Networks With STDP-Based Unsupervised Pre-training Followed by Supervised Fine-Tuning. *Frontiers in Neuroscience*, 12, 2018.
- [5] Jingren Zhang, Jingjing Wang, Xie Di, and Shiliang Pu. High-Accuracy and Energy-Efficient Action Recognition with Deep Spiking Neural Network. In *Neural Information Processing (ICONIP)*, pages 279–292, 2022.
- [6] Wei Fang, Zhaofei Yu, Yanqi Chen, Tiejun Huang, Timothée Masquelier, and Yonghong Tian. Deep Residual Learning in Spiking Neural Networks. In *Advances in Neural Information Processing Systems*, volume 34, pages 21056–21069. Curran Associates, Inc., 2021.
- [7] Mireille El-Assal, Pierre Tirilly, and Ioan Marius Bilasco. 2D versus 3D Convolutional Spiking Neural Networks Trained with Unsupervised STDP for Human Action Recognition. In *International Joint Conference on Neural Networks (IJCNN) 2022*, Padova, Italy, July 2022.
- [8] Mireille El-Assal, Pierre Tirilly, and Ioan Marius Bilasco. A Study On the Effects of Pre-processing On Spatio-temporal Action Recognition Using Spiking Neural Networks Trained with STDP. In *International Workshop on Content-based Multimedia Indexing (CBMI)*, 2021.
- [9] Jiarong Chen, Zongqing Lu, and Qingmin Liao. XSepConv: extremely separated convolution for efficient deep networks with large kernels. In *International Conference on Digital Image Processing (ICDIP 2021)*, volume 11878, June 2021.
- [10] Andrew G. Howard, Menglong Zhu, Bo Chen, Dmitry Kalenichenko, Weijun Wang, Tobias Weyand, Marco Andreetto, and Hartwig Adam. MobileNets: Efficient Convolutional Neural Networks for Mobile Vision Applications. *CoRR*, abs/1704.04861, 2017.
- [11] Mark Sandler, Andrew Howard, Menglong Zhu, Andrey Zhmoginov, and Liang-Chieh Chen. Mobilenetv2: Inverted residuals and linear bottlenecks. In *International Conference on Computer Vision and Pattern Recognition*, pages 4510–4520, 2018.
- [12] Christian Schuldt, Ivan Laptev, and Barbara Caputo. Recognizing Human Actions: A Local SVM Approach. In *Proceedings of the Pattern Recognition, 17th International Conference on (ICPR'04) Volume 3 - Volume 03, ICPR '04*, page 32–36, USA, 2004. IEEE Computer Society.
- [13] Lena Gorelick, Moshe Blank, Eli Shechtman, Michal Irani, and Ronen Basri. Actions as space-time shapes. *Transactions on Pattern Analysis and Machine Intelligence*, 29(12):2247–2253, December 2007.
- [14] Daniel Weinland, Rémi Ronfard, and Edmond Boyer. Free viewpoint Action Recognition Using Motion History Volumes. *Computer Vision and Image Understanding*, 104(2-3):249–257, 2006.
- [15] Romain Belmonte, Nacim Ihaddadene, Pierre Tirilly, Ioan Marius Bilasco, and Chaabane Djeraba. Video-Based Face Alignment With Local Motion Modeling. In *Winter Conference on Applications of Computer Vision (WACV)*, pages 2106–2115, 2019.
- [16] Moez Baccouche, Franck Mamalet, Christian Wolf, Christophe Garcia, and Atilla Baskurt. Sequential Deep Learning for Human Action Recognition. In B. Lepri A.A. Salah, editor, *2nd International Workshop on Human Behavior Understanding (HBU)*, pages 29–39, Amsterdam, Netherlands, November 2011. Springer.
- [17] Kensho Hara, Hirokatsu Kataoka, and Yutaka Satoh. Can Spatiotemporal 3D CNNs Retrace the History of 2D CNNs and ImageNet? *CoRR*, abs/1711.09577, 2017.
- [18] Christoph Feichtenhofer, Haoqi Fan, Jitendra Malik, and Kaiming He. SlowFast Networks for Video Recognition. In *International Conference on Computer Vision (ICCV)*, October 2019.
- [19] Christoph Feichtenhofer. X3D: Expanding Architectures for Efficient Video Recognition. *CoRR*, abs/2004.04730, 2020.
- [20] J. Arunehru, G. Chamundeswari, and S. Prasanna Bharathi. Human Action Recognition using 3D Convolutional Neural Networks with 3D Motion Cuboids in Surveillance Videos. *Procedia Computer Science*, 133:471–477, 2018. International Conference on Robotics and Smart Manufacturing (RoSma2018).
- [21] Du Tran, Lubomir D. Bourdev, Rob Fergus, Lorenzo Torresani, and Manohar Paluri. Learning Spatiotemporal Features With 3D Convolutional Networks. In *International Conference on Computer Vision (ICCV)*, 2015.
- [22] Alexandre Lacoste, Alexandra Luccioni, Victor Schmidt, and Thomas Dandres. Quantifying the Carbon Emissions of Machine Learning. *CoRR*, abs/1910.09700, 2019.
- [23] Emma Strubell, Ananya Ganesh, and Andrew McCallum. Energy and Policy Considerations for Deep Learning in NLP. In *Proceedings of the 57th Annual Meeting of the Association for Computational Linguistics*, pages 3645–3650, Florence, Italy, July 2019. Association for Computational Linguistics.
- [24] François Chollet. Xception: Deep learning with depthwise separable convolutions. In *International Conference on Computer Vision and Pattern Recognition*, pages 1251–1258, 2017.
- [25] D. Tran, H. Wang, L. Torresani, J. Ray, Y. LeCun, and M. Paluri. A Closer Look at Spatiotemporal Convolutions for Action Recognition. In *International Conference on Computer Vision and Pattern Recognition (CVPR)*, pages 6450–6459, Los Alamitos, CA, USA, jun 2018. IEEE Computer Society.
- [26] Mike Davies, Narayan Srinivasa, Tsung-Han Lin, Gautham China, Yongqiang Cao, Sri Harsha Choday, Georgios Dimou, Prasad Joshi, Nabil Imam, Shweta Jain, Yuyun Liao, Chit-Kwan Lin, Andrew Lines, Ruokun Liu, Deepak Mathaikuttu, Steven McCoy, Arnab Paul, Jonathan Tse, Guruguhanathan Venkataramanan, Yi-Hsin Weng, Andreas Wild, Yoonseok Yang, and Hong Wang. Loihi: A Neuromorphic Manycore Processor with On-Chip Learning. *IEEE Micro*, 38(1):82–99, 2018.
- [27] Anthony Burkitt. A Review of the Integrate-and-fire Neuron Model: I. Homogeneous Synaptic Input. *Biological cybernetics*, 95:1–19, 2006.
- [28] Catherine D. Schuman, Thomas E. Potok, Robert M. Patton, J. Douglas Birdwell, Mark E. Dean, Garrett S. Rose, and James S. Plank. A Survey of Neuromorphic Computing and Neural Networks in Hardware. *ArXiv*, abs/1705.06963, 2017.
- [29] Zahra Babaiee, Ramin M. Hasani, Mathias Lechner, Daniela Rus, and Radu Grosu. On-Off Center-Surround Receptive Fields for Accurate and Robust Image Classification. In *International Conference on Machine Learning (ICML)*, pages 1–21, 2021.
- [30] Pierre Falez. *Improving Spiking Neural Networks Trained with Spike Timing Dependent Plasticity for Image Recognition*. Ph.d. thesis, Université de Lille, 2019.
- [31] Bhaskar Chakraborty, Michael Holte, Thomas Moeslund, Jordi González, and Xavier Roca. A Selective Spatio-temporal Interest Point Detector for Human Action Recognition in Complex Scenes. In *International Conference on Computer Vision (ICCV)*, pages 1776–1783, 2011.
- [32] Shuiwang Ji, Wei Xu, Ming Yang, and Kai Yu. 3D Convolutional Neural Networks for Human Action Recognition. *IEEE Transactions on Pattern Analysis and Machine Intelligence*, 35(1):221–231, 2013.
- [33] Andrew Howard, Mark Sandler, Bo Chen, Weijun Wang, Liang-Chieh Chen, Mingxing Tan, Grace Chu, Vijay Vasudevan, Yukun Zhu, Ruoming Pang, Hartwig Adam, and Quoc Le. Searching for MobileNetV3. In *International Conference on Computer Vision (ICCV)*, pages 1314–1324, 2019.
- [34] Pierre Falez, Pierre Tirilly, Ioan Marius Bilasco, Philippe Devienne, and Pierre Boulet. Unsupervised Visual Feature Learning with Spike-timing-dependent Plasticity: How Far are We From Traditional Feature Learning Approaches? *Pattern Recognition*, 93:418–429, 2019.
- [35] Pierre Falez, Pierre Tirilly, Ioan Marius Bilasco, Philippe Devienne, and Pierre Boulet. Mastering the Output Frequency in Spiking Neural Networks. In *International Joint Conference on Neural Networks (IJCNN)*, 2018.